Image Artifacts in Very Low Magnetic Field MRI: the Role of Concomitant Gradients

D. A. Yablonskiy[1], A. L. Sukstanskii[1], J. J. Ackerman[1]
[1]Mallinckrodt Institute of Radiology, Washington University, St. Louis, MO, United States

Introduction: Increasing interest in MRI with hyperpolarized gases (see, for example, [1, 2]), which can produce a large MR signal even at low magnetic fields, has lead to attempts to build MRI scanners that employ very low magnetic fields (several mT [3-5]). While MRI at very low magnetic fields has certain potential advantages, it may also face problems that are not encountered with MRI at high field (0.1 – 10 T). This presentation is concerned with one set of these problems – artifacts resulting from concomitant magnetic field gradients unavoidably created by the gradient coils used to encode spatial information in MRI.

Background: Any static magnetic field $\mathbf{b}(\mathbf{r})$ in a free space satisfies Maxwell's equations $\nabla\cdot\mathbf{b}(\mathbf{r})=0,\quad \nabla\times\mathbf{b}(\mathbf{r})=0$. It immediately follows that an inhomogeneous magnetic field cannot have a single non-zero component. Consider the usual inhomogeneous Z-axis magnetic field $b_z = G_x x + G_y y + G_z z$ employed in MRI. The actual magnetic field also includes concomitant inhomogeneous components $b_x = -0.5G_z x + G_x z$ and $b_y = 0.5G_z y + G_y z$ [6] with the same amplitude as the B_Z gradients. Gradients as strong as 10-20 mT/m are typically used in human imaging experiments. Hence, transverse magnetic fields as strong as 5-10 mT will also be present (FOV about 0.5 m). Therefore, in a very low field scanner (several mT or even µT), the transverse concomitant magnetic field may be on the order of or even larger than B_0. Consequently, the local Larmor angular frequency becomes $\omega = \gamma\left[(B_0+b_z)^2+(b_x)^2+(b_y)^2\right]^{1/2}$.

Geometrical Image Distortions: Magnetic field gradients are broadly used in MRI for different purposes: slice selection, phase and frequency encoding, etc. Consider <u>*slice selection*</u> along the direction *x* perpendicular to the main field $\mathbf{B}_0$, which requires application of gradient $b_z = G_x x$ and is necessarily accompanied by the concomitant field $b_x = G_x z$. In the idealized absence of concomitant field $G_x z$, a RF pulse of frequency ω would excite spins along a plane $x = x_0$, where x_0 satisfies the condition $\gamma(B_0 + G_x x_0) = \omega$. However, the unavoidable presence of the concomitant field yields selection profile coordinates satisfying the condition $(x-x_c)^2 + z^2 = R_x^2,\quad R_x = |x_0 + B_0/G_x|,\quad x_c = -B_0/G_x$ rather than the plane $x = x_0$. This surface is a cylinder of radius R_x with an axis parallel to the *Y*-axis crossing through the point $\{x_c = -B_0/G_x,\ 0, 0\}$. The "targeted" plane $x = x_0$ is tangential to the cylinder. Note also that the position of the cylinder's axis is independent of x_0, i.e., independent of the RF slice-selection frequency ω. Thus, RF pulses with different slice-selection frequencies excite not a set of parallel planes but a set of *concentric* cylinders of different radii. As a result, a targeted slice of a thickness Δx_0 "deforms" into an annulus between two cylinders; a cross section of this annulus being a ring of the same thickness Δx_0. The deviation of the points on the cylinder's surface from the targeted plane, δx, depends on their *z*-coordinate. If the field B_0 is strong enough, the distortion parameter $\varepsilon = G_x L / B_0$ is small and only a small portion of the circle resides within the FOV (*L*). However, if the field B_0 is small enough and $\varepsilon \sim 1$, the situation is different and the entire circle may reside within the FOV. The situation with plane selection along the *Y*-axis is similar to the *X*-axis. To get corresponding results, in all above-derived equations one should substitute *x* by *y*. However, if the targeted slice is selected along the *Z*-axis so that gradient $b_z = G_z z$ is applied, it will be accompanied by concomitant field components b_x and b_y that transform the targeted plane into an ellipsoid $(z-z_c)^2 + (x^2+y^2)/4 = R^2$, where $z_c = -B_0/G_z,\quad R_z = |z_0 - z_c|$. <u>*Read-out*</u> and <u>*phase-encoding*</u> procedures yield geometrically similar considerations, producing relationships between targeted objects and obtained MR data.

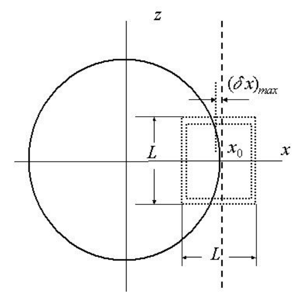

Intensity Image Distortions: The presence of concomitant fields also leads to an inhomogeneous distribution of magnetization in the selected curved "slice". Indeed, by the end of the slice-selection gradient ramp-up period, spins will have aligned along the direction of magnetic field (we assume that adiabatic condition holds). Because of the presence of concomitant gradients, this field is inhomogeneous in both magnitude and orientation, application of a slice-selecting RF pulse will then also create a rather complex and spatially dependent distribution of magnetization orientation, thus ultimately signal intensity, within the selected curved slice. Next, during the read-out procedure, when the gradient is on, a time-dependent *z*-component of magnetization **M** appears in addition to the desired transverse components. Also, the absolute value of the projection of **M** on the *XY*-plane becomes time-dependent; hence, a standard interpretation of magnetization rotating in the transverse plane is no longer valid.

Conclusion: This presentation derives expressions describing geometrical relationships between the imaged object and the obtained MR data. At very low field the concomitant field gradients that are inevitably generated by the same gradient coils that generate desired gradients used in MRI for spatial encoding cause substantial geometric and intensity deformations of imaged objects. If unaccounted for, corresponding image distortions will create substantial difficulties in very low field MR image interpretation. An obvious solution to the problems of MRI at very low fields is to use imaging gradients with very low amplitudes. In this case, the image deformation parameter ε can be made small, preserving the accuracy of the image's geometrical parameters. However, this approach substantially impairs imaging capabilities. Another possible approach is to use relationships derived herein to restore the shape of original object.

Acknowledgement: This work is supported in part by NIH grants R01-NS41519, R01-HL70037, R24-CA83060 and P30 CA91842.

1. Leawoods, J.C., et al., Concepts Magn Reson, 2001. **13**(5): p. 277-293. 2. Moller, H.E., et al., Magn Reson Med, 2002. **47**(6): p. 1029-51. 3. Tseng, C.H., et al., Phys Rev Lett, 1998. **81**(17): p. 3785-8. 4. Venkatesh, A.K., et al., Magn Reson Imaging, 2003. **21**(7): p. 773-6. 5. Bidinosti, C.P., et al., J Magn Reson, 2003. **162**(1): p. 122-32. 6. Norris, D.G. and J.M.S. Hutchinson, Magn. Reson. Imag., 1990. **8**: p. 33-37.